Electron-Nuclear Double Resonance of Ag Nuclei in AgCl+Fe^{3+}†

MITSUO SATOH* AND CHARLES P. SLICHTER
Department of Physics and Materials Research Laboratory, University of Illinois, Urbana, Illinois
(Received 15 November 1965)

The electron nuclear double resonance (ENDOR) spectra of both isotopes ^{107}Ag and ^{109}Ag have been measured at 1.3°K in a single crystal of silver chloride containing 0.0006% Fe^{3+} ions. The angular variation of the ENDOR spectrum agrees with that calculated from the tetrahedral model proposed by Hayes, Pilbrow, and Slifkin in which the iron ion occupies the interstitial site, the four nearest-neighbor silver ions being absent. The superhyperfine structure (super-hfs) constants of the second, third, and fourth neighbor ^{107}Ag and ^{109}Ag nuclei with the magnetic electrons in the ferric iron were obtained together with the directions of their principal axes. The isotropic hf interactions are probably due to indirect $\mathbf{I}\cdot\mathbf{S}$ couplings between the neighboring Ag nuclei and the magnetic electrons on the ferric iron via conduction electrons in the excited states.

I. INTRODUCTION

ELECTRON paramagnetic resonance (EPR) measurements on Fe^{3+} ions in iron-doped silver halide crystals which had been annealed in a halogen atmosphere have been reported by Hennig,[1,2] by Hayes, Pilbrow, and Slifkin,[3] and by Garth[4]. The spectrum of the ferric iron in AgCl has a cubic symmetry and g is isotropic:

$$g=2.015\pm0.002, \quad (1)$$

$$a=(76\pm4)\times10^{-4}\ \mathrm{cm}^{-1}. \quad (2)$$

Hayes *et al.*[3] observed a partially resolved super-hfs on the central line of the five-line spectrum and suggested from its analysis that the ferric ions occupy the interstitial sites in the AgCl crystal, forming a tetrahedral complex $(FeCl_4)^-$. In order to avoid a large excess positive charge, this model requires the association of the ferric iron with four nearest-neighbor silver-ion vacancies.

Garth[4] showed from the angular dependence of the chlorine ENDOR spectrum at 1.3°K that the cubic spectrum of Fe^{3+} ions in AgCl is due to the iron situated at the center of a tetrahedron formed by four nearest-neighbor chlorine ions along [111] and equivalent directions from the iron. In addition, he obtained hf and quadrupole constants of ^{35}Cl and ^{37}Cl nuclei which explain the complete chlorine ENDOR spectrum from 6 to 24 Mc/sec.

There are three models[4] of the ferric iron center with tetrahedral symmetry which are consistent with Garth's ENDOR data.

(1) One is the tetrahedral complex model proposed by Hayes *et al.* as stated above.

(2) Another is a model in which the iron ion is located at an interstitial site surrounded by four chlorine and four silver nearest neighbors which form two tetrahedrons. The net charge of this center is $+3e$. This model, however, is less likely than the other two, because the crystallographic inversion symmetry requires a small cubic crystalline potential, while the observed cubic field splitting parameter "a" is the value of Eq. (2) and is as large as that for ferric iron in the typical octahedral and tetrahedral sites.[5,6]

(3) Another model with the same tetrahedral symmetry is that formed by substituting an $(FeCl_4)^-$ complex for a Cl^- ion at a normal chlorine lattice site. The center of this model has no net charge and, hence, requires no vacancies to compensate its charge. But the complex is probably too big for the available space without excessive lattice strain. To determine which of the three tetrahedral models cited above is correct, further ENDOR experiments for more distant nuclei than the nearest-neighbor chlorine are required.

This paper reports a study of ENDOR spectra at 1.3°K. The lines observed correspond to the second, third, and fourth neighbor ^{107}Ag and ^{109}Ag nuclei in AgCl single crystal containing Fe^{3+} ions. These lines are compared with the theoretical curves derived from each model cited above. It is then concluded that the interstitial model (1) suggested by Hayes *et al.* is correct, and many hfs constants of the neighboring silver nuclei and the directions of their principal axes are calculated upon the basis of this model. The isotropic super-hf interaction is explained as an indirect $\mathbf{I}\cdot\mathbf{S}$ coupling between the neighboring Ag nuclei and the d electrons in the ferric iron via conduction electrons in the excited states.

II. EXPERIMENTAL

The silver chloride single crystals used in this study were the same samples as Garth used in his experiments. Details of preparation are given in his paper.[4] The rectangular sample, 16 mm×9mm×2mm, was cut

† Work supported in part by the U. S. Atomic Energy Commission under Contract AT(11-1)-1198.
* On leave of absence from Okayama University, Okayama, Japan.
[1] K. Hennig, Phys. Status Solidi **3**, K458 (1963).
[2] K. Hennig, Phys. Status Solidi **7**, 885 (1964).
[3] W. Hayes, J. R. Pilbrow, and L. M. Slifkin, J. Phys. Chem. Solids **25**, 1417 (1964).
[4] J. C. Garth, Ph.D. thesis, University of Illinois, 1965 (unpublished); also Phys. Rev. **140**, A656 (1965).
[5] W. Low, *Paramagnetic Resonance in Solids* (Academic Press Inc., New York, 1960), p. 119.
[6] S. Geschwind, Phys. Rev. **121**, 363 (1961); R. S. Title, *ibid.* **131**, 623 (1963).

with faces parallel to a (100) plane and edges parallel to the [100] axis in this plane.

All runs of ENDOR were carried out at 1.3°K using a superheterodyne X-band spectrometer, built originally by Holton and Blum[7] and modified to lock the klystron frequency onto that of the sample cavity.[8] The angular variation of the ENDOR frequencies was performed by rotating the magnet to change the angle θ between the external field and one of the cubic crystal axes. The ENDOR lines were observed on each of the five EPR transitions with the magnetic field set to the absorption peak of each transition.

The range of the ENDOR frequency studied in this experiment was from 390 to 6400 kc/sec. From the magnitude of the "field shift"[4] of the ENDOR lines, it was found that all ENDOR lines from 390 to 900 kc/sec arise from the silver nucleus, and the assignment of silver isotopes and M_s values (the eigenvalues of the electron spin) of individual ENDOR lines were carried out at $\theta=90°$ (see Appendix).

III. EXPERIMENTAL RESULTS AND ANALYSIS

The spin Hamiltonian for $Fe^{3+}(3d^5,{}^6S_{5/2})$ in AgCl which has a cubic symmetry is

$$\mathcal{H}=g\beta\mathcal{H}_0\cdot\mathbf{S}+(a/6)[S_{x'}{}^4+S_{y'}{}^4+S_{z'}{}^4-\tfrac{1}{5}S(S+1)\times(3S^2+3S-1)]+\sum\mathcal{H}_{Cl}+\sum\mathcal{H}_{Ag}, \quad (3)$$

where $S=\frac{5}{2}$ and $x'y'z'$ directions denote axes of the cubic field. The first term represents the electronic Zeeman interaction; the second, the effect of the crystal field of cubic symmetry. The third term describes the interactions of nearest-neighbor chlorine nuclei (Cl-hf,-nuclear-Zeeman and -quadrupole interactions) and has already been discussed in connection with the central super-hfs of five fine-structure splittings of the EPR spectrum[3] and ENDOR lines of ^{35}Cl and ^{37}Cl nuclei.[4] It is the last term containing the Ag-hf and Ag-nuclear Zeeman interaction that is mainly discussed in this study. The summations in Eq. (3) run over the pairs of isotopes ^{35}Cl, ^{37}Cl, and ^{107}Ag, ^{109}Ag, respectively.

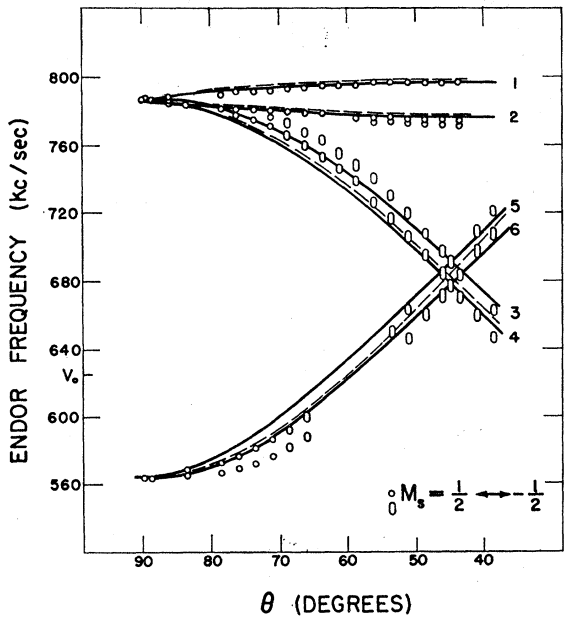

FIG. 1. The angular dependence of the ENDOR spectrum of the second-neighbor ^{109}Ag nuclei corresponding to $M_s=\frac{1}{2}$. The solid and dashed curves are calculated using model 1 ($\sigma=2$) and model 3 ($\sigma=1$), respectively.

[7] W. C. Holton and H. Blum, Phys. Rev. **125**, 89 (1962).

[8] The spectrometer was modified by J. C. Bushnell to lock the klystron frequency onto that of the sample cavity.

The part of the complete spin Hamiltonian of the system which depends upon one isotope of Ag nuclei will be

$$\mathcal{H}_{Ag}=\sum_\sigma\sum_j(-\gamma_n\hbar\mathbf{H}_0\cdot\mathbf{I}_{\sigma j}+A_{\sigma x}I_{\sigma jx}S_x+A_{\sigma y}I_{\sigma jy}S_y+A_{\sigma z}I_{\sigma jz}S_z), \quad (4)$$

where the first term is the silver nuclear Zeeman term and the others are the super-hf interaction of the jth Ag nucleus in the σth shell of neighbors with magnetic electrons of the ferric iron, and x, y, z represent the principal axes of the latter interaction. γ_n values are negative for both ^{107}Ag and ^{109}Ag nuclei.

A. First Shell ($\sigma=1$)

There were no experimental ENDOR lines[9] whose angular variation corresponded to the nearest-neighbor Ag nuclei, for either the case of an interstitial complex or that of the substitutional model. Therefore, it is recognized that the nearest-neighbor Ag^+ ions are missing, and the model (2) cited in the Introduction is not the case.

B. Second Shell ($\sigma=2$)

At first the calculation will be performed according to model (1)—the interstitial complex model. If an Fe^{3+} ion is located at an interstitial site $(a/2,a/2,a/2)$ in the lattice, where a is the lattice distance of AgCl, then twelve members of the second-neighbor Ag^+ ion will be described as

$$j=\binom{1}{2}:\frac{a}{2}(\pm1,-3,\pm1),\quad j=\binom{7}{8}:\frac{a}{2}(\pm3,\ 1,\mp1),$$

$$j=\binom{3}{4}:\frac{a}{2}(\mp1,\ 3,\pm1),\quad j=\binom{9}{10}:\frac{a}{2}(\pm1,-1,\pm3),$$

$$f=\binom{5}{6}:\frac{a}{2}(\pm3,-1,\pm1),\quad j=\binom{11}{12}:\frac{a}{2}(\mp1,\ 1,\pm3),$$

where $(a/2)(+1,-3,+1)$ and $(a/2)(-1,-3,-1)$ express $j=1$ and $j=2$, respectively, and so forth. When the external field is rotated in the $x'z'$ plane and makes

[9] In this study the frequency range of the ENDOR oscillator covered up to 6.4 Mc/sec, and Garth's experiment was in the range between 1 and 24 Mc/sec. Then we confirmed this.

an angle θ with the z' axis of the cubic symmetry, the squares of the resonance frequencies of the second neighbor Ag nucleus appropriate to $M_s=\frac{1}{2}$ can be derived by the use of Eq. (4):

$$\begin{pmatrix}\nu_{1,2}^2\\ \nu_{3,4}^2\end{pmatrix}=\nu_0^2+X\alpha_2^2(\cos\theta\pm\sin\theta)^2+Y\gamma_2^2(\cos\theta\pm\sin\theta)^2 +\frac{Z}{2}(\cos\theta\mp\sin\theta)^2,$$

$$\begin{pmatrix}\nu_{5,6}^2\\ \nu_{7,8}^2\end{pmatrix}=\nu_0^2+X(\alpha_2\cos\theta\pm\beta_2\sin\theta)^2 +Y(\delta_2\cos\theta\mp\gamma_2\sin\theta)^2+\frac{Z}{2}\cos^2\theta, \quad (5)$$

$$\begin{pmatrix}\nu_{9,10}^2\\ \nu_{11,12}^2\end{pmatrix}=\nu_0^2+X(\beta_2\cos\theta\pm\alpha_2\sin\theta)^2 +Y(\gamma_2\cos\theta\mp\delta_2\sin\theta)^2+\frac{Z}{2}\sin^2\theta,$$

with

$$X=\nu_0A_{2x}/h+A_{2x}^2/4h^2,$$
$$Y=\nu_0A_{2y}/h+A_{2y}^2/4h^2, \quad (6)$$
$$Z=\nu_0A_{2z}/h+A_{2z}^2/4h^2,$$

where the (+,+,−) and the (−,−,+) sequences correspond to $\nu_{1,2}^2$ and $\nu_{3,4}^2$, respectively, and so on; the subscripts on the left side of Eq. (5) represent the jth member of the set of second neighbors; α_2, β_2, γ_2, and δ_2 describe[10] the direction cosines of principal axes of the super-hf interaction ($\sigma=2$), with respect to the cubic axes $x'y'z'$; and ν_0 is the silver nuclear resonance frequency in the external field alone. Equation (5) gives the resonance frequencies of each isotope of Ag if all the ν_0 and hf constants are substituted in.

Figure 1 shows the angular variation of the second neighbor ^{109}Ag ENDOR spectrum at 1.3°K corresponding to $M_s=\frac{1}{2}$ with the magnetic field set to the absorption peak of the $M_s=\frac{1}{2}\leftrightarrow-\frac{1}{2}$ transition, where the solid lines are calculated curves based upon the interstitial complex model (1) as will be described later, and the circles and ellipses (showing the peak-to-peak derivative line widths) represent the observed ENDOR frequencies.

As seen in Fig. 1, there are, in general, six ENDOR frequencies at an arbitrary angle, which, however, reduce to a smaller number at $\theta=45°$ and $\theta=90°$. By a selection of four distinct frequencies at any one angle, the constants A_2's, α_2, β_2, etc., can be found[10] from Eqs. (5) and (6). We have chosen rather to use as four frequencies line 1 at 45° and 90°, and line 5 at 45° and 90°. This choice also permits a unique evaluation of

[10] For instance, for $j=1$, $(a/2)(1,-3,1)$ we have a principal axis of the direction $(-1/\sqrt{2},0,1/\sqrt{2})$. When the other principal axes are taken such as $(\alpha_2,-\beta_2,\alpha_2)$ and $(\delta_2,\gamma_2,\delta_2)$, there are three relations: $2\alpha_2^2+\beta_2^2=1$, $2\delta_2^2+\gamma_2^2=1$, and $2\alpha_2\delta_2-\beta_2\gamma_2=0$. Since the number of unknown constants in Eq. (5) and Eq. (6) is 7, four more equations which can be derived from Eq. (5) with 4 ENDOR frequency values, are necessary to solve the problem.

TABLE I. Super-hyperfine constants[a] and directions of principal axes of the neighboring Ag nuclei.

σ	Nucleus	$A_{\sigma x}$ (kc/sec)	$A_{\sigma y}$ (kc/sec)	$A_{\sigma z}$ (kc/sec)	γ	$\cos^{-1}\alpha_\sigma$ (deg)	$\cos^{-1}\beta_\sigma$ (deg)	$\cos^{-1}\delta_\sigma$ (deg)	$\cos^{-1}\gamma_\sigma$ (deg)	a_σ (kc/sec)	$b_{\sigma x}$ (kc/sec)	$b_{\sigma y}$ (kc/sec)	$b_{\sigma z}$ (kc/sec)	$A_{\sigma p}$ (kc/sec)	$A_{\sigma p}'$ (kc/sec)
2	^{109}Ag	302.5 ±1.9	342.0 ±2.0	−123.1 ±2.0		88.07 ±0.3	2.7 ±0.06	45.07 ±0.2	87.28 ±0.3	173.8 ±2.0	128.7 ±2.0	168.2 ±2.0	−296.9 ±2.0	37.94	173.0
2	^{107}Ag	260.5 ±1.5	296.0 ±2.0	−107.6 ±1.6		87.7 ±0.3	4.05 ±0.1	45.07 ±0.2	86.73 ±0.3	149.6 ±1.7	110.9 ±1.6	146.4 ±2.0	−257.2 ±1.8	32.99	150.5
2	^{109}Ag/^{107}Ag	1.16	1.15	1.14	1.15					1.16	1.16	1.15	1.15		
3	^{109}Ag	28.0 ±1.8	36.6 ±0.7	−29.5 ±0.6		46.0 ±0.6	78.8 ±1.5	82.0 ±0.8	11.2 ±0.9	11.7 ±1.0	16.3 ±2.0	24.9 ±1.0	−41.2 ±0.9	16.7	33.3
3	^{109}Ag	22.0 ±1.4	36.8 ±0.9	−24.0 ±0.6		46.3 ±0.9	77.7 ±1.2	81.4 ±1.0	12.3 ±0.8	11.6 ±1.0	10.4 ±1.6	25.2 ±1.2	−35.6 ±1.0		
4 (j=1–12)	^{109}Ag	12.0 ±1.4	21.6 ±0.8	−27.3 ±0.7		71.9 ±0.8	26.0 ±0.4	50.6 ±0.4	64.0 ±0.6	2.1 ±1.0	9.9 ±1.4	19.5 ±1.0	−29.4 +1.0	9.86	15.5
4 (j=13–16)	^{109}Ag	22.0 ±1.4	22.0 ±1.4	−44.0 ±2.8		54.7 ± 0.6	54.7 ± 0.6	65.9 ± 0.8	35.3 ± 0.6	0 ±0.5	22.0 ±1.6	22.0 ±1.8	−44.0 ±3.0	9.86	33.3
		28.0 ±1.8	28.0 ±1.8	−56.0 ±3.6							28.0 ±2.0	28.0 ±1.8	−56.0 ±3.8		

[a] The values divided by h are shown on the table.

the constants. They are tabulated on Table I, where

$$A_{\sigma\xi}=a_\sigma+b_{\sigma\xi}, \quad (\xi=x,y,z),$$
$$\sum_{\xi=x,y,z} b_{\sigma\xi}=0, \tag{7}$$

with a_σ the contact hf constants of S electron, and $b_{\sigma\xi}$ the anisotropic hf constants.

It is remarkable that A_{2z} and b_{2z} are negative and the others positive, $\alpha_2\approx\gamma_2\approx 0$, $\beta_2\approx 1$, and roughly $b_{2x}\approx b_{2y}$, in both Ag isotopes. This means that the z principal axis of the hf interaction of the second-neighbor Ag nuclei points nearly toward the nearest-neighbor Cl^- ion rather than the Fe^{3+} center, with near axial symmetry around this axis. The solid curves of Fig. 1 are derived from these constants again by the use by Eqs. (5) and (6), and they coincide fairly well with the experimental points. The observed frequencies near $\theta=90°$ and 45° coincide with the theoretical values; however, at the other angles the former have slight deviations from the latter which exceed the experimental errors. In the last section this departure will be discussed. In the frequency range from 606 to 642 kc/sec, no lines of the second-neighbor Ag nuclei could be observed because they were lost in the numerous signals of the third and fourth neighbors.

Next, model (3), the substitutional complex model which was referred to at the end of the Introduction, will be considered. Now, if we take the nearest-neighbor Ag^+ ions into consideration, the dashed curves in Fig. 1 are obtained in a way similar to the abovementioned procedure. When the two models are compared, the interstitial one (model 1) clearly coincides with the experimental facts and is therefore the correct one, inasmuch as it possesses the same number of lines (6) as there are experimental lines in Fig. 1, while the substitutional model (model 3) has a smaller number (4). If we take the second-neighbor Ag nuclei of the substitutional model to explain the experiment, the calculation gives only four curves and very different behavior from the empirical angular variations in Fig. 1. The hf interaction of $\sigma=3$ and 4, which will be discussed below, also supports this result. Because the number of lines is a function of the symmetry of the center and largely independent of the details of analysis, we consider this argument to give powerful support to the interstitial model.

In this experiment the silver nuclear Zeeman interaction was always larger than the Ag-hf coupling (for the ^{109}Ag nucleus, $\nu_0=625$ kc/sec, while the largest hf constant $A_{2y}/h=342$ kc/sec in Table I). Therefore, the angular variation of the ^{109}Ag ENDOR spectrum ($\sigma=2$) appropriate to $M_s=-\frac{1}{2}$ was obtained as a reflection pattern of the spectrum in Fig. 1 with respect to a symmetrical line $\nu_0=625$ kc/sec. The second-neighbor ENDOR spectra of another isotope, ^{107}Ag, corresponding to both $M_s=\frac{1}{2}$ and $-\frac{1}{2}$ were observed in the range from 390 to 700 kc/sec, with $\nu_0=544.0$ kc/sec and the same features as with ^{109}Ag ($\sigma=2$), but with a little smaller frequency spread to the spectrum because γ is smaller than for ^{109}Ag nuclei. The constants of the ^{107}Ag hf interaction, etc. are also summarized on Table I. As expected, Table I shows that the ratios of hf constants of ^{109}Ag and ^{107}Ag nuclei are nearly equal to $\gamma_{Ag^{109}}/\gamma_{Ag^{107}}$, and the directions of principal axes of the two nuclei coincide precisely with each other within an experimental error of angle 80′.

C. Third and Fourth Shells ($\sigma=3$ and 4)

Figures 2 and 3 show the ENDOR lines due to the third- and fourth-neighbor ^{109}Ag nuclei appropriate to $M_s=-\frac{1}{2}$, respectively; the points represent the experimental angular variations at the transitions $M_s=\frac{1}{2}\leftrightarrow-\frac{1}{2}$ and $-\frac{1}{2}\leftrightarrow-\frac{3}{2}$ (in the latter, the frequencies were reduced to that of the former for convenience) and the calculated curves are based upon the interstitial model (1), $\sigma=3$ and 4 of Figs. 2 and 3, respectively. Similar figures were also obtained for the isotope ^{107}Ag around $\nu_0=544.0$ kc/sec.

The calculated curves due to the interstitial complex model (1) and the experimental frequencies coincide with one another in these figures, while the substitutional model (3) has an angular dependence distinctly different from that found in Figs. 2 and 3, even though we try various assignments of shells ($\sigma=2$, 3, and 4). Therefore, the model (1) gives the correct result for

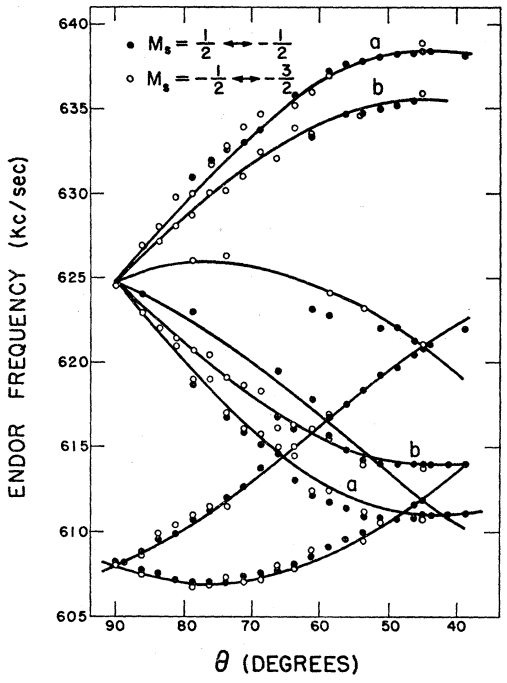

FIG. 2. The angular variation of the ENDOR frequency of the third-neighbor ^{109}Ag nuclei appropriate to $M_s=-\frac{1}{2}$. The solid curves are calculated from model 1 ($\sigma=3$). For curves (a) and (b) see the text.

these data, as was also the case for the second shell ($\sigma=2$).

The rows $\sigma=3$ and 4 in Table I show the hf constants and the directions of their principal axes calculated by a way similar to that for $\sigma=2$. In the case $\sigma=4$, there are two groups of silver nuclear members denoted as $j=1$–12 and $j=13$–16, in which the ions of the latter group are situated along the [111] direction (they have an exactly axially symmetric hf interaction), so the hf constants of these two groups are independent of one another. One of the curves (a) and (b) in Figs. 2 and 3 corresponds to four members of $\sigma=3$; the other corresponds to the $j=13$–16 members of $\sigma=4$. However, since both curves have the same angular dependence,

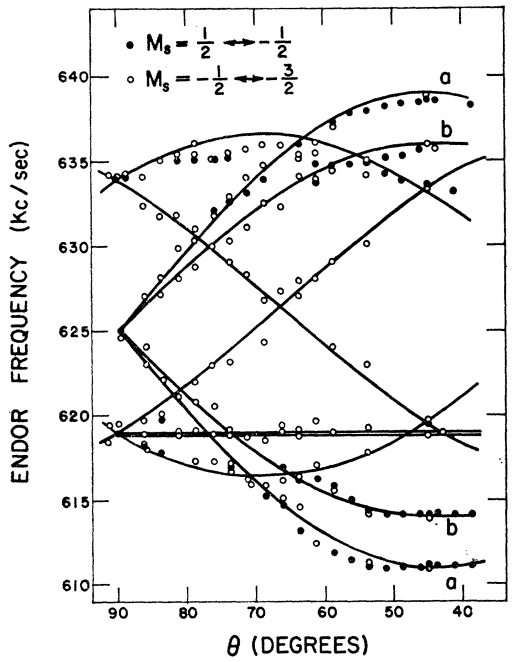

FIG. 3. The angular dependence of the ENDOR lines of the fourth-neighbor ^{109}Ag nuclei corresponding to $M_s=-\frac{1}{2}$. The solid curves are calculated using model 1 ($\sigma=4$). For curves (a) and (b) see the text.

preventing a unique assignment, two sets of constants are given on the line $\sigma=3$ and $\sigma=4$, $j=13$–16 in Table I.

D. Analysis of the hf Constants

The values of $A_{\sigma p}$ in Table I represent the anisotropic hf couplings calculated from the direct magnetic dipole-dipole interaction of the σth neighbor Ag nuclei with the unpaired electrons at the ferric iron in the state $M_s=\frac{1}{2}$. The values of $A_{\sigma p}'$ represent the corresponding calculation assuming the entire unpaired electron spin to be located at the nearest-neighbor Cl^- sites. The latter calculation is a great overestimate of the effect of covalency in the models with a complex

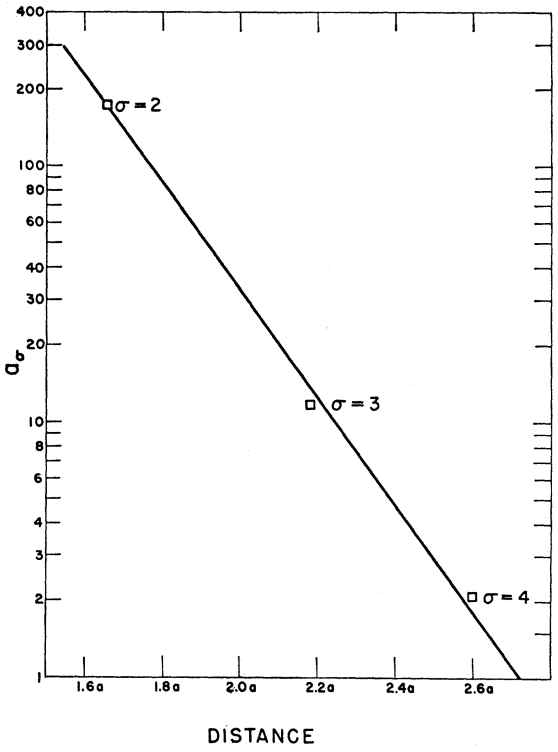

FIG. 4. The isotropic super-hyperfine constants of neighboring ^{109}Ag nuclei versus the distance from Fe^{3+} ion to the σth-neighbor ^{109}Ag nucleus. a is 2.76 Å, the lattice distance of the AgCl crystal.

center $(FeCl_4)^-$ (models 1 and 3). Since these overestimates of the $A_{\sigma p}'$'s are of the same order as those for the b_σ's, we believe there must be a contribution from the pseudodipolar coupling.

The values a_σ in Table I are the isotropic super-hfs constants derived from the values of experimentally determined A_σ's using Eq. (7), with $\sigma=2$, 3, and 4. It is unlikely that this interaction is a direct-contact hf coupling, because the magnetic electrons in the ferric iron extend over at most nearest-neighbor Cl^- sites. Figure 4 shows the decay of a_σ with distance R_σ between the ferric iron center and the σth neighbor Ag site. It is closely exponential with distance.

Many workers have investigated the indirect nuclear-nuclear, nuclear-electron, or electron-electron spin exchange interaction via S electrons of the conduction band in a metal,[11] insulator,[12] alloy,[13] ferromagnetic insulator,[14] and so forth. It is our belief that the coupling of the Ag to the Fe^{3+} is via this mechanism. The interaction may be described as an indirect $\mathbf{I}\cdot\mathbf{S}$ coupling of the σth neighbor Ag nuclei with the d electrons in ferric iron via electrons in the AgCl energy bands. On this mechanism there will be an effective interaction energy

[11] M. A. Ruderman and C. Kittel, Phys. Rev. **96**, 99 (1954).
[12] N. Bloembergen and T. J. Rowland, Phys. Rev. **97**, 1679 (1955).
[13] K. Yoshida, Phys. Rev. **106**, 893 (1957).
[14] J. Callaway, Nuovo Cimento **25**, 625 (1962).

between the Fe^{3+} and the silver which is given in second-order perturbation theory:

$$\sum_{k,k';s,s'} \frac{(Fksm|\mathcal{H}_{Bd}|F'k's'm)(F'k's'm|\mathcal{H}_{I\sigma B}|F'ksm')}{E_k-E_{k'}}+\text{C.C.}, \tag{8}$$

where $\mathcal{H}_{Bd}$ represents an interaction between a d electron in the ferric iron and an electron in one of the bands of the AgCl lattice, and $\mathcal{H}_{I\sigma B}$ represents the hf coupling of the σth Ag nucleus with the same band electron, and where F and s describe the eigenvalues of the electron spin on the iron and in the band, and m the Ag nuclear spin. The summation over the band states is to be taken over all ground states k and excited states k' and the two spin orientations s'. If one assumes a very narrow valence band and a broad conduction band, the isotropic hf constants a_σ can be found[12] from Eq. (8) as

$$\ln(a_\sigma/a_{\sigma'})=\hbar^{-1}(2m^*E_g)^{\frac{1}{2}}(R_\sigma-R_{\sigma'}), \tag{9}$$

where m^* is the effective mass of the conduction electron and E_g the energy gap from the appropriate valence band to the conduction band. It is most likely that the important states will involve wave functions which are large primarily near silver sites, because they will have in their excited state a large S character at the Ag nuclei, as is needed for an isotropic hf coupling. Such functions should also couple strongly to the Fe^{3+} d electrons, since the ground-state functions should still be large at the vacant silver sites adjacent to the iron. The band structure of AgCl crystals shows[15–19] $E_g\approx 6.6$ eV, if one assumes the highest filled band made up of silver atomic functions is the ground electronic state. Using this value for E_g and the slope of the line in Fig. 4, the value m^* can be obtained from Eq. (9) as about $2m_e$, where m_e is the free-electron mass. Although this value may be somewhat larger than the other data,[20] it is entirely reasonable for such a crude calculation.

IV. DISCUSSION

A small deviation of the measured ENDOR frequency of the second-neighbor Ag nuclei from the calculated curves appears on each line, except for 1 and 2, in Fig. 1, as described above. This departure exceeds the experimental errors because the maximum deviation is about 13 kc/sec, while the individual ENDOR frequency could be measured within an error of about 0.5 kc/sec and the calculated curves contain an error of maximum about 4 kc/sec owing to the experimental errors of about 0.5 kc/sec at four base points.[10] The angular dependence of the deviation is roughly $\sin^n 4\theta$, where n is an integer. This dependence may be derived when a second-order perturbation of the cubic crystal field with off-diagonal terms of the hf interaction is taken into consideration; it produces a mixing between the neighboring nuclear energy levels.[21,22] The correction is of the order of several kc/sec at $\theta=3\pi/8$ in curves 3 and 4, and is a little smaller than the observed value, about 13 kc/sec. This interaction also shows that curves 1 and 2 should have corrections of the same order. However, a correction of the order of several kc/sec is contained within the empirical error. Consequently, although this interaction will exist, it cannot explain these deviations.

The second-order hf interaction was calculated and is of the order of only 10 cps, owing to small hf constants.

The terms such as S^-, S^{3+}, etc. of the cubic crystal field operator affect also the position of ENDOR lines,[21] and give $\sin^2 4\theta$ angular dependence. However, these interactions have an effect of the order of only 100 cps in our case.

Though the effect of tilting of the axis of electron quantization from the external field direction due to the crystal field was considered, this amounts to only $(a/6\beta H_0)\sin 4\theta\approx 0.4$ cps at $\theta=3\pi/8$.

The high-order terms of the Hamiltonian such as $H_xI_x^3+H_yI_y^3+H_zI_z^3$ may be considered[23]; however, such a term gives a different angular variation from $\sin^n 4\theta$.

Accordingly, the small deviation in Fig. 1 has not been explained at present.

ACKNOWLEDGMENTS

This work was carried out during the tenure of a Research Associateship at the University of Illinois, Urbana, Illinois, by one of us (M. S.). He wishes to express his gratitude to the members of this Institution for their hospitality. We especially thank J. H. Pifer and Dr. J. C. Garth for their experimental advice and valuable discussions.

APPENDIX

From the magnitude of the "field shifts"[4] of the ENDOR lines, it was found that all ENDOR lines

[15] Y. Okamoto, Nachr. Akad. Wiss. Göttingen, II Math. Physik. Kl. **275** (1956).
[16] F. Seitz, Rev. Mod. Phys. **23**, 328 (1951).
[17] F. C. Brown, T. Masumi, and H. H. Tippins, J. Phys. Chem. Solids **22**, 101 (1961); F. C. Brown, J. Phys. Chem. **66**, 2368 (1962).
[18] F. Bassani, R. S. Knox, and W. B. Fowler, Phys. Rev. **137**, A1217 (1965).
[19] P. M. Scop, Solid State and Molecular Theory Group, MIT, Quarterly Progress Report No 54, 1964 (unpublished), p. 15; P. M. Scop, Phys. Rev. **139**, A934 (1965).
[20] F. C. Brown and F. E. Dart, Phys. Rev. **108**, 281 (1957).
[21] T. P. P. Hall, W. Hayes, and F. I. B. Williams, Proc. Phys. Soc. (London) **78**, 883 (1961).
[22] J. E. Drumheller and R. S. Rubins, Phys. Rev. **133**, A1099 (1964).
[23] J. M. Baker and F. I. B. Williams, Proc. Roy. Soc. (London) **A267**, 283 (1962).

TABLE II. The assignment of nuclear species and M_s of individual ENDOR lines. ($\theta=90°$).

ν (kc/sec) for $M_s=\frac{1}{2}\leftrightarrow-\frac{1}{2}$	$\Delta\nu$ (kc/sec)	ν (kc/sec) for $M_s=\frac{1}{2}\leftrightarrow\frac{3}{2}$	$\Delta\nu$ (kc/sec)	$\frac{1}{3}\Delta\nu$ (kc/sec)	ν (kc/sec) for $M_s=-\frac{1}{2}\leftrightarrow-\frac{3}{2}$	$\Delta\nu$ (kc/sec)	$\frac{1}{3}\Delta\nu$ (kc/sec)	Assignment of isotope and M_s
405.2	−138.8±0.3							107, $-\frac{1}{2}$
464.6	−160.4±0.3							109, $-\frac{1}{2}$
					465.0	−42.2±0.3	−14.1±0.1	107, $-\frac{3}{2}$
491.2	−53.2±0.3	523.8	−53.4±0.3					107, $+\frac{1}{2}$
529.5	−14.5±0.3				492.8	−14.4±0.3		107, $-\frac{1}{2}$
		553.5	−23.5±0.4	−7.8±0.1				107, $+\frac{3}{2}$
536.5	−7.5±0.4	569.4	−7.8±0.4					107, $+\frac{1}{2}$
539.0	−5.0±0.4				502.3	−4.9±0.3		107, $-\frac{1}{2}$
544.0	0	577.2	0		507.2	0		107, (center)
548.9	+4.9±0.4	582.3	+5.1±0.4					107, $+\frac{1}{2}$
551.5	+7.5±0.4				515.3	+8.1±0.3		107, $-\frac{1}{2}$
					531.5	+24.3±0.3	+8.1±0.1	107, $-\frac{3}{2}$
558.2	+14.2±0.4	592.0	+14.8±0.6					107, $+\frac{1}{2}$
563.8	−61.2±0.4	602.6	−61.5±0.6					109, $+\frac{1}{2}$
		620.0	+42.8±0.6	+14.3±0.2				107, $+\frac{3}{2}$
		636.5	−27.6±0.6	−9.3±0.2				109, $+\frac{3}{2}$
597.2	+53.2±0.6				560.2	+53.0±0.4		107, $-\frac{1}{2}$
607.9	−17.1±0.6				567.0	−16.8±0.4		109, $-\frac{1}{2}$
615.3	−9.3±0.6	655.0	−9.1±0.6					109, $+\frac{1}{2}$
618.9	−6.1±0.6				577.5	−6.3±0.6		109, $-\frac{1}{2}$
625.0	0	664.1	0		583.8	0		109, (center)
630.8	+5.8±0.6	669.5	+5.4±0.6					109, $+\frac{1}{2}$
634.0	+9.0±0.6				592.5	+8.7±0.6		109, $-\frac{1}{2}$
641.8	+16.8±0.6	681.0	+16.9±0.6					109, $+\frac{1}{2}$
		713.5	+49.4±0.6	+16.5±0.2				109, $+\frac{3}{2}$
683.1	+139.1±0.6	716.0	+138.8±0.7					107, $+\frac{1}{2}$
686.8	+61.8±0.6							109, $-\frac{1}{2}$
785.8	+160.8±0.6	825.0	+160.9±0.7					109, $+\frac{1}{2}$

from 390 to 900 kc/sec were due to the silver and not the chlorine nucleus. In Table II, ν represents the measured ENDOR frequency at $\theta=90°$ and $\Delta\nu$ means $\nu-\nu_0$, the difference between ν and the nuclear resonance frequency ν_0 in the external field alone, where

$^{109}\nu_0=625.0$ kc/sec, $^{107}\nu_0=544.0$ kc/sec
for $M_s=\frac{1}{2}\leftrightarrow-\frac{1}{2}$,

$^{109}\nu_0=664.1$ kc/sec, $^{107}\nu_0=577.2$ kc/sec
for $M_s=\frac{1}{2}\leftrightarrow\frac{3}{2}$,

and

$^{109}\nu_0=583.8$ kc/sec, $^{107}\nu_0=507.2$ kc/sec
for $M_s=-\frac{1}{2}\leftrightarrow-\frac{3}{2}$.

Since the silver nuclear Zeeman energy is larger than the hf coupling in this experiment (see text), a symmetry of lines with respect to ν_0 and the comparison of $\Delta\nu$ between each electronic transition enable us to assign the isotope species and M_s values of individual ENDOR lines.